Numerical Simulation of Weld Thermal Efficiency GTAW Process

Mouad Bensada[1](✉), Abdellah Laazizi[1], Kaoutar Fri[1], and Jamal Fajoui[2]

[1] SECNDCM-L2MC, ENSAM-Moulay Ismail University, Meknes, Morocco
{mouad.bensada,plek.fri,k.fri}@edu.umi.ac.ma,
a.laazizi@ensam.umi.ac.ma
[2] GeM, IUT-Saint Nazaire 44600, Saint-Nazaire, France
Jamal.Fajoui@univ-nantes.fr

Abstract. Predicting temperature field in a Gas Tungsten Arc Welding process is essential and precondition for any study of thermal or mechanical behavior of the weld. In fact, thermal, material proprieties and physical phenomena have to be taken into account in order to predict welding morphology, residual stresses and the final product quality of the weld. In the case of analytical studies, simulations are done with many simplifications that affect result precision. In this study, a 2D numerical model is developed by taking into account heat transfer and distribution of heat source. Gaussian distribution for heat source is presented and simulated by using Finite Difference Method (FDM) with explicit scheme. This method permits following the evolution of temperature field throughout the studied material during welding process. Also, operating parameters effects on melted zone such as current welding and shielding gas have been discussed.

Keywords: GTAW process · Numerical simulation · Welding · Shielding gas · Explicit scheme

1 Introduction

The use of welding as joining process replacing riveting permits to minimize the weight of structure either in the automotive or the aeronautic industries [1], it contributes also in reducing the production cost. Gas Tungsten Arc Welding (GTAW) is widely used in many industrial applications, it is characterized by high welding quality, compared to other arc welding processes [2]. Therefore, predicting temperature field and controlling defect creation are important for any preventive study of the GTAW process parameters [3]. In addition, temperature gradients are considered one of the main parameters that affects the microstructure of the welded materials then their final mechanical proprieties. As a result, thermal proprieties and physical phenomena have to be taken into consideration in order to predict welding morphology, residual stresses and the final product quality of the welds [4].

Last decade, it has been challenging to simulate the welding behaviors in whole piece because of software requirements and long computational time [5].

© The Author(s), under exclusive license to Springer Nature Switzerland AG 2023
L. Azrar et al. (Eds.): CIP 2022, LNME, pp. 353–362, 2023.
https://doi.org/10.1007/978-3-031-23615-0_36

The aim of the current research is to develop a 2D model of GTAW process by including heat source distribution and the heat transfer. Finite difference method is used to solve numerical model. The effect of welding operating parameters such as welding current and shielding gas are discussed.

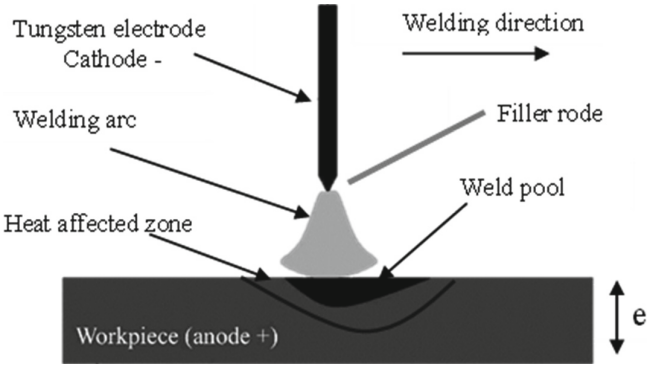

Fig. 1. GTAW process presentation

Nomenclature			
C_p	Specific heat (J/Kg.K)	T(t, x, z)	Temperature (°C)
e	Thickness of workpiece(mm)	T_o	Initial temperature, 25 (°C)
h_{conv}	Heat transfer coefficient	t	Time (s)
I	welding current (A)	v	Welding source velocity (m/s)
k	Thermal conductivity (W/m.K)	V	Welding voltage (V)
L	Length of workpiece	x, z	Cartesian coordinats (m)
UTS	Ultimate tensile strength(MPa)	σ	Standard deviation
Q_m	Welding input source (W/m^2)	η	Welding process efficiency
r	radial distance of the Gaussian function (m)	ρ	Density (Kg/m^3)

2 GTAW Process Modeling

As seen in Fig. 1, a non-consumable tungsten electrode is used to create the weld, the tungsten electrode does not melt. An electric arc is produced between the work piece and the tungsten electrode, the heating could reach a temperature up to 19.400 °C [6]. The inert shielding gas is utilized to protect the melted zone and the welding electrode from atmospheric oxidation. GTAW is widely appreciated in fields requiring precision, such as chemical, aircraft and nuclear industry [7].

Rosenthal [8] has been the first to develop an analytical model to calculate temperature distribution during welding by using simplifying assumptions. Heat source was considered as a punctual source with a constant velocity. The calculated temperature field was:

$$T = T_0 + \exp\left(\frac{-vX}{2K}\right)\psi(x, y, z) \tag{1}$$

With 'T0' is the initial temperature, (x, z) is the coordinate of the punctual heat source, 'v' is the velocity of the heat source and $\boldsymbol{\Psi}(\mathbf{x}, \mathbf{z})$ is a function to be defined.

In the case of the thin plate, one of the most known solutions is [9]:

$$T = T_0 + \frac{\frac{q}{v}}{e(4\pi\lambda\rho ct)^{1/2}} \exp\left(\frac{-r^2}{4Kt}\right) \tag{2}$$

where 'e' is the thickness of the plate, 'q' is the welding power and 't' is time. The heat source and melted zone were considered moving with a velocity 'v' and a length 'l' [10].

Nunes [11] has proposed an extended Rosenthal weld model, the temperature field 'T' represented approximately as following:

$$T = T_0 + q\left[F(n = 0) + \sum_{n=1}^{\infty}\left(F(r_n) + F\left(r'_n\right)\right)\right] \tag{3}$$

where 'F' is a function to be defined.

Therefore, modelling the heat source as a punctual source does not allow determining the maximal temperature near to the heat source centre, which limits the comparison between the experimental and the analytical study.

3 Heat Source Modelling

In this study, the spatial distribution of the power welding input has been taken into account. The heat source is presented as a Gaussian function distribution as centred normal law with a radial distance 'R', standard deviation '$\sigma = 0.4$'. Figure 2 shows the used heat source distribution [12].

An axisymmetric 2D of a GTAW model is considered. The heat input is depending to the voltage 'V', the current 'I' and the efficiency of the welding process 'η'.

By assuming the energy distribution is Gaussian, the absorbed energy flux on the top surface ($z = 0$) is given as:

$$Q_m = \frac{VI\eta}{2\psi^2}\exp\left(\frac{-R^2}{2\sigma^2}\right) \tag{4}$$

In the case of GTAW the process efficiency "η" takes into account the heat absorption coefficient, since this process is characterized by the presence of an inert gas that protects the molten area. In general, in this process with an inert gas composed of 82% Ar and 18% CO_2, the efficiency of the process is equal to 80% [13].

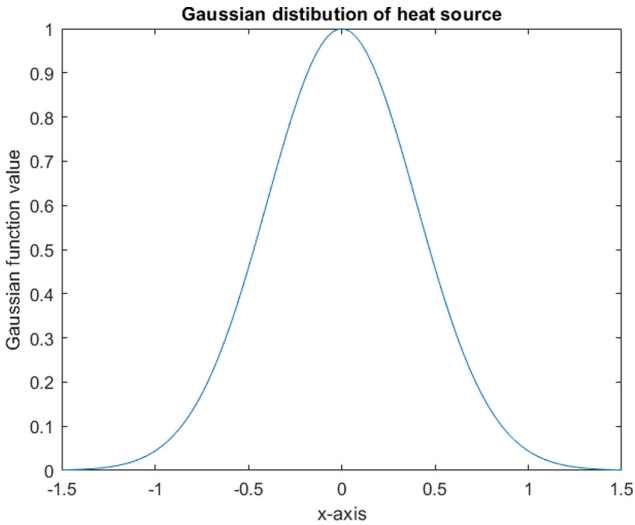

Fig. 2. Heat source presentation

4 Heat Transfer Modeling in GTAW Process

Nowadays, steel is considered as one of the most preferable materials in automotive application due to low cost comparing to others metallic materials. A new generation of high strength steel is now used in the automotive field offering a high capacity of fuel efficiency, enhanced safety a good formability characteristic. Mild 140/270 steel is employed principally on the fuel tank of the car, the structure is assembled by GTAW process, the main characteristic of the used materiel is presented in Table 1.

In this numerical study, a 2D dimensional model is introduced as a plat with a thickness 'e' and width 'L'.

Table 1. Material properties of mild steel

Steel grade	Yield strength (MPa)	UTS (MPa)	Density (Kg/m^3)	K (W/m.K)	Cp (J/K.kg)	hconv ($W/m^2.K$)
Mild 140/270	140	270	7200	25	300	40

The heat source of welding 'Q_m' has been introduced as a boundary condition (Table 2) in addition to the conviction exchange with the air (Eq. 6).

The governing equations are presented as follow:

$$\rho Cp\frac{\partial T}{\partial t} = k\left(\frac{\partial^2 T}{\partial x^2}+\frac{\partial^2 T}{\partial z^2}\right) \tag{5}$$

The upper surface is in contact with air, it submitted to convective heat transfer as shown below:

$$-k\frac{\partial T}{\partial z} = h_{conv}(T - T_0) + Q_m \tag{6}$$

Cartesian geometry was used; the x–z plane was taken for the surface of the work piece that absorbs the heat generated by electric arc. The length and thickness of the studied piece were 5×5 mm^2 respectively.

In order to enhance the accuracy of calculation, the finite difference method was used to solve numerically the mathematical model (5) and (6). The explicit scheme is applied. It builds up an iterative calculation in time. As a result, the temperature is written as:

$$T(t+1, j, k) = T(t, j, k) + \frac{\Delta t}{\rho Cp}\left[\frac{T(t, j-1, k) - 2T(t, j, k) + T(t, j, k)}{\Delta x^2} + \frac{T(t, j, k-1) - 2T(t, j, k) + T(t, j, k+1)}{\Delta z^2}\right] \tag{7}$$

However, the explicit scheme has to respect the following relation (Eq. 8) in order to be stable. For this reason, the choice of Δt is limited:

$$\frac{\Delta t}{\rho Cp}\left(\frac{1}{\Delta x^2} + \frac{1}{\Delta z^2}\right) \leq 1/2 \tag{8}$$

Although the timescale required the use of fine grids and very small-time steps to obtain accurate results, that will lead to longer calculation time. The space grid was taking as $\Delta x = \Delta z = 0.1$ mm.

In this current study, the welding source Q_m was included as Neumann boundary condition. For both lateral surfaces were considered at 25 °C. The model has been developed and simulated in MATALB environment.

Table 2. Boundary conditions of the work piece

Position	Boundary conditions
x = 0	T = T0
x = L	T = T0
z = 0	$-k\frac{\partial T}{\partial z} = h_{conv}(T - T_0) + Q_m$

5 Results

Figure 3 illustrate the problem-solving flowchart concerning the overall iterative approach for the calculation of temperature field during GTAW process in all points of the workpiece, temperature was calculated at every step of time by using finite difference

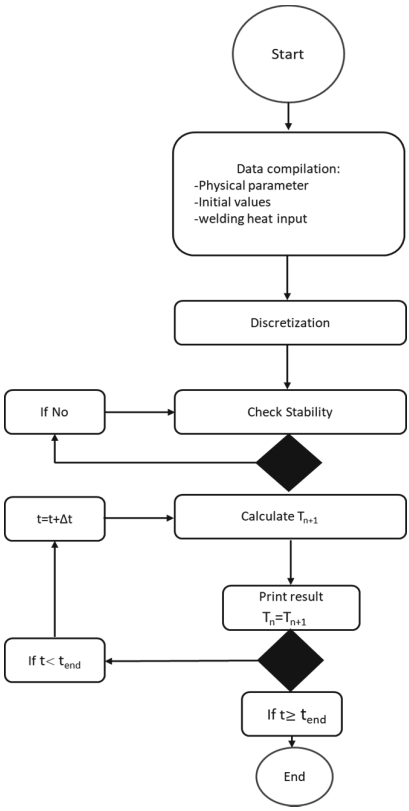

Fig. 3. Problem solving flowchart

method and by checking stability condition at every point of the work piece, then calculate the temperature until finishing the welding time. Figure 4 shows the temperature field after 10 s of GTAW process with current I = 90 A and voltage V = 10 V.

Using Isotherm diagram (Fig. 5), it was possible to calculate the dimension of the melted zone, for I = 90A and U = 10V, we have the width = 4.4 mm and depth = 0.7 mm.

With a V = 15 V and according to the Fig. 6, varying welding parameters, especially the welding current, affect the dimension of the melted zone. In fact, Increasing the welding current, leads to the growth of the melted zone.

6 Comparison with Experimental Study

In order to ensure of the validity of the developed model, it was necessary to compare with experimental results. KERRICH [14] has studied the effects of various welding parameters on the GTAW process and specially the welding current on the penetration of the melted zone in a structural steel. They showed that increasing the welding current leads to the growth of the melted zone which was in good agreement with the corresponding numerical calculation.

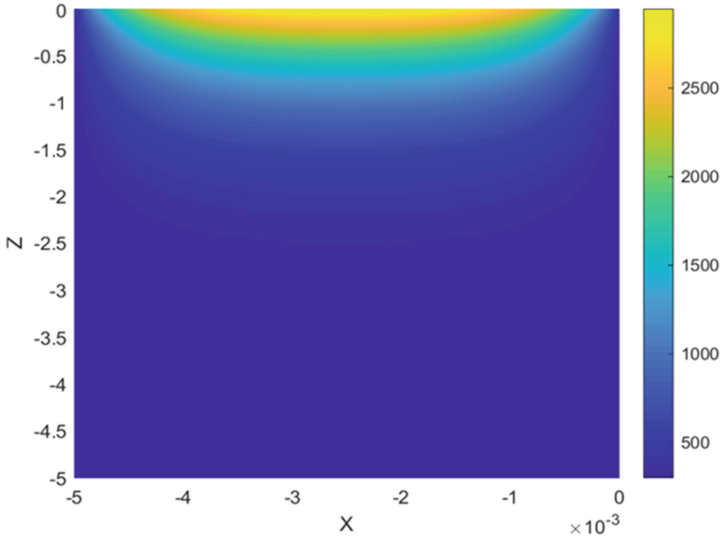

Fig. 4. Temperature field after 10 s of welding process I = 90A, U = 10V

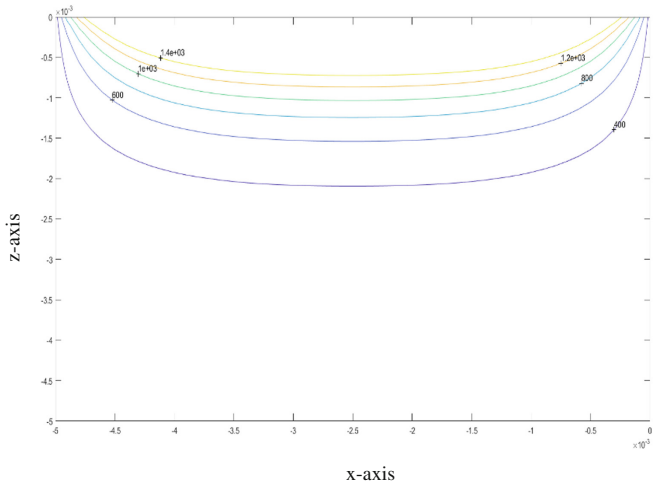

Fig. 5. Isotherm diagram for I = 90 A, V = 10V

According to the Table 3 the comparison with the experimental study reveals a slight difference in terms of the depth of the melted zone, this can be explained by the simplifying assumptions taken in the numerical study including that the weld pool movement were not taking into account.

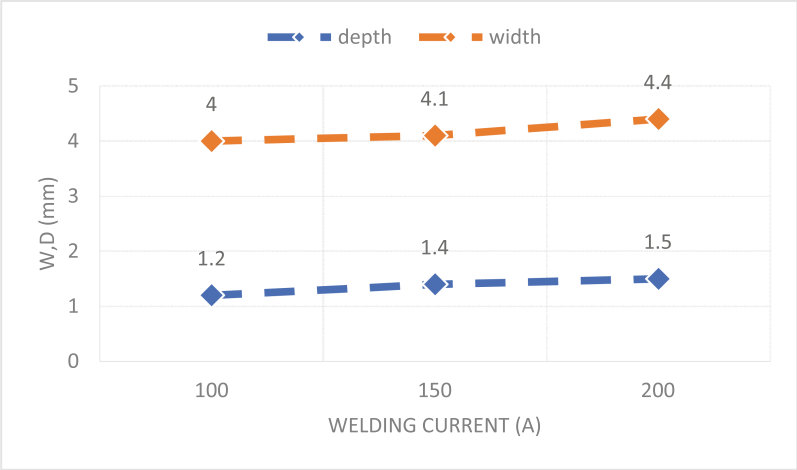

Fig. 6. Evolution of the melted zone dimensions versus welding current.

Table 3. Comparison between experimental and numerical welding penetration

Arc voltage (V)	Welding current (A)	Experimental penetration (mm) [12]	Numerical penetration (mm)
10	180	1.3	1.4
	210	1.8	1.6
	300	2.1	1.8

7 Effect of the Shielding Gas Rate on the Weld Penetration

Due to its inert chemical reactivity with weld pool, Argon (Ar) is used as shielding gas [15]. The effect of gas flow rate of Ar was studied by Anbarasan [16]. He proved that increasing the shielding gas rate leads to the decrease of the process efficiency.

In order to discuss the effect of shielding gas rate on the weld penetration, two values of the process efficiency are implemented in the numerical model (Table 4).

Table 4. Weld penetration in function of the process efficiency

Efficiency	Weld penetration (mm)
0.5	0.5
0.9	0.8

According to the Table 4, increasing the process efficiency leads to the growth of the weld penetration, which mean that increasing the shielding gas rate decrease the weld penetration.

8 Conclusion

A numerical model of GTAW process has been developed to analyze the effect of the welding current and shielding gas rate on the temperature distributions and the shape of weld pool. Finite Difference Method with explicit scheme was used, including a description of a gaussian heat source distribution.

Computational results showed that increasing intensity leads to the growth of the melted zone, which may induce high residual stress and risks of metal failure.

Comparison with experimental results was made in terms of welding penetration. The behavior of measured widths of the fusion zone was in good agreement with the numerical calculations. These analyses can be used to optimize the GTAW power and the efficiency of the process. As an extension of the present research work, we pretend to take into account the weld pool movement in calculating temperature field and simulate the thermal stress.

References

1. Laazizi, A., et al.: Applied multi-pulsed laser in surface treatment and numerical–experimental analysis. J. Opt. Laser Tech. **43**(7), 1257–1263 (2011)
2. Traidia, A.: Multiphysics modelling and numerical simulation of GTA weld pools. PhD thesis Ecole Polytechnique Paris (2011)
3. Zhu, X.K., Chao, Y.J.: Effects of temperature-dependent material properties on welding simulation. J. Comput. Struct. **80**, 967–976 (2002). https://doi.org/10.1016/S0045-7949(02)00040-8
4. Rong, Y., Xu, J., Huang, Y., Zhang, G.: Review on finite element analysis of welding deformation and residual stress. J. Sci. Technol. Welding Joining **23**(3), 198–208 (2018). https://doi.org/10.1080/13621718.2017.1361673
5. Tao, J., Zhang, T.C., Liu, P.T., Li, J.: Numerical computation of a linear friction welding process. J. Mater. Sci. Forum **575–578**, 811–815 (2008). https://doi.org/10.4028/www.scientific.net/msf.575-578.811
6. Kutelu, B.J., Seidu, S.O., Eghabor, G.I., Ibitoye, A.I.: Review of GTAW welding parameters. J. Minerals Mater. Charact. Eng. **6**, 541–554 (2018). https://doi.org/10.4236/jmmce.2018.65039
7. Subodh, K., Shahi, A.S.: Effect of heat input on the microstructure and mechanical properties of gas tungsten arc welded AISI 304 stainless steel joints. Mater. Des. **32**, 3617–3623 (2011). https://doi.org/10.1016/j.matdes.2011.02.017
8. Rosenthal, D.: Mathematical theory of heat distribution during welding and cutting. J. Welding. **20**, 220–234 (1941)
9. Poorhaydari, K., Patchett, B.M., Ivey, D.: Estimation of cooling rate in the welding of plates with intermediate thickness. J. Suppl. Welding. (2005)
10. Song, S., Pei, X., Dong, P.: Analytical interpretation of welding linear heat input for 2d residual stress models. In: ASME 2015 Pressure Vessels and Piping Conference. https://doi.org/10.1115/PVP2015-45753
11. Nunes, Jr. A.C.: An extended Rosenthal weld model. J. Welding J. (1983)
12. Mazuco, F., Teixeira, P.R., Bezerra de Araújo, D.: Two heat source models to simulate welding processes with magnetic deflection. Soldagem & Inspeção (2017)
13. Karadeniz, E., Ozsarac, U., Yildiz, C.: The effect of process parameters on penetration in gas metal arc welding processes. J. Mater. Des. **28**, 649–656 (2007)

14. Kerrich, D.: Contribution a l'etude du parametrage du procede de soudage tig (sans métal d'apport et avec apport de fil chaud): application aux cas des eprouvettes tubulaires. phd thesis universite des sciences & techniques de lille. (1997)
15. Kah, P., Martikainen, J.: Influence of shielding gases in the welding of metals. 1411–1421 (2013). https://doi.org/10.1007/s00170-012-4111-6
16. Anbarasan, N., Jerome, S.: Effect of flow rate and argon-hydrogen shielding gas mixture on weld bead morphology of inconel 718. Mater. Today: Proc. **5**(2018), 26990–26996 (2018). https://doi.org/10.1016/j.matpr.2018.09.002